# AERODYNAMICS OF A TWISTED WALL JET IN A CO-CURRENT FLOW

É. P. Volchkov, N. A. Dvornikov, and V. I. Terekhov

UDC 536.524

Twisted wall jets are used fairly often in different vortical-type devices – ejectors, centrifugal separators and classifiers, swirl tubes, etc. Under actual conditions, such flows are usually co-current flows, and in the general case the companion flow also has a rotational component.

Below we examine two types of twisted flows – a jet flowing about a cylinder (external problem, Fig. 1), and a jet developing in a cylindrical channel (internal problem). The main difference between these schemes can be explained as follows. In the external part of the jet flowing over the cylinder ($\delta_m < y < b$, Fig. 1), circulation decreases with an increase in radius ($\partial\Gamma/\partial r < 0$). In accordance with Rayleigh's principle of stability, there should then be an intensification of transport processes. However, turbulent exchange is suppressed in the boundary region of this jet ($0 < y < \delta_m$). The effect of body forces is the opposite in the case of the jet developing in the channel. In the external part of this jet, where $\partial\Gamma/\partial r > 0$, turbulent pulsations are reduced and turbulent transport is diminished. This has been confirmed by the results of measurements of the turbulence structure of twisted wall jets [1, 2].

Calculation of aerodynamically semi-infinite twisted jets is a complex problem. The main difficulties encountered in the theoretical analysis stem from the three-dimensional character of the flow, as well as the need to allow for the effect of centrifugal forces on the intensity of turbulent transport. The literature does not contain any solutions of such problems which have allowed for the entire complex of factors to be considered.

Integral methods [3, 4] have been widely used in calculations of untwisted semi-infinite jets. Being simple, they usually give finite analytic formulas and, with an accuracy sufficient for practical purposes, coincide with the experimental results in regard to the main parameters – friction, heat transfer, and integral characteristics. Similar methods can also be used to analyze twisted wall jets. Here, to solve integral relations for linear and angular momenta, energy, and mass transfer, it is necessary to establish similarity profiles of longitudinal and circumferential velocity and the laws governing the expansion of the jet and the change in the maximum values of the velocity components along the cylinder in the flow or along the channel. The present study is devoted to theoretical determination of these quantities. We will examine the case of flow with an injection parameter $m = \rho_s w_s / \rho_0 w_0 > 1$. The results of the calculations are compared with experimental data.

1. Similarity Profiles of the Longitudinal and Circumferential Components of Velocity in the Jet. As a rule, in integral methods of calculation [3, 4], the jet is subdivided into two regions – the boundary region ($0 < y < \delta_m$) and the external region ($\delta_m < y < b$). The velocity profiles in the external part are described by the relations characteristic of free turbulence, while the profiles in the boundary region are characterized by the relations for a boundary layer. In analyzing complex three-dimensional semi-infinite wall jets, it is more convenient to use a single relation which describes the velocity profile over the entire cross section of the jet.

We will seek the velocity profile in the form of a superposition of functions which account for the development of the boundary layer $f_b(\xi, w_{m0})$ and rest of the jet $g(\xi, w_0, w_{m0})$, where $\xi = y/b$, $w_{m0}$ is the maximum velocity in the section in the absence of momentum loss to friction against the wall:

$$w = w_{m0} f_b(\xi, w_{m0}) g_c(\xi, w_0, w_{m0}). \quad (1.1)$$

We assign the function $f_b$ in the form of a power profile of velocity $f_b = (y/\delta)^n$, while we assign $g_c$ as a linear combination of the Schlichting jet profile:

Novosibirsk. Translated from Zhurnal Prikladnoi Mekhaniki i Tekhnicheskoi Fiziki, No. 6, pp. 67-74, November-December, 1987. Original article submitted July 9, 1986.



0021-8944/87/2806-0864$12.50 

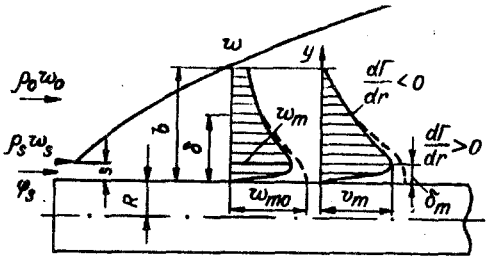


Fig. 1

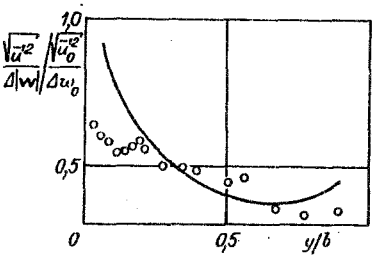


Fig. 2

$$g_c = a_1(1 - \xi^{1,5})^2 + a_2. \tag{1.2}$$

Using the boundary conditions ($g_c = 1$ at $\xi = 0$ and $g = w_0/w_{m0}$ at $\xi = 1$), we write the profile of longitudinal velocity in the submerged wall jet in the form

$$w = w_{m0}\xi^n (b/\delta)^n \left[\left(1 - \frac{w_0}{w_{m0}}\right)(1 - \xi^{1,5})^2 + \frac{w_0}{w_{m0}}\right], \tag{1.3}$$

where $\delta$ is the thickness of the boundary layer over which the effect of the wall is felt. Its value can be found by solving the integral momentum equation for a turbulent boundary layer with longitudinally-curved streamlines [5] $\delta = 0.37(w_{m0}x/\nu)^{-0.2}\Psi^{0.8}$.

Under quasi-isothermal conditions $T_w/T_0 \approx 1$, the relative friction function is determined by an increase in flow velocity and the effect of the body forces on turbulent transport $\Psi = \Psi_\varphi \Psi_к$. Since the velocity in (1.3) is weakly dependent on $b/\delta$, in determining $\delta$ we can ignore the dependence on relative curvature, having set $\Psi = \Psi_\varphi = \cos\varphi^{-0,75}$.

In the absence of a companion flow ($w_0 = 0$), Eq. (1.3) is similar to the Karman profile [6] used to describe secondary radial flow on a rotating disk. At $w_0/w_{m0} = 1$, Eq. (1.3) becomes the power velocity profile; it should be noted that Wormley's profile [7] for end flow in a swirl chamber does not yield such an asymptote. At $w_0/w_{m0} > 1$, Eq. (1.3) describes the velocity profile in wall gas screens ($m < 1$).

The coordinate of the velocity maximum in profile (1.3) is found from

$$\xi_m = \delta_m/b = \left[P_1 - \sqrt{P_1^2 - P_2}\right]^{2/3} \tag{1.4}$$

or $\xi_m = 1$ if $w_0/w_{m0} > 0.834$, $P_1 = \frac{1.5 + n}{3 + n}$, $P_2 = \frac{n}{(3+n)(1 - w_0/w_{m0})}$.

It can be seen that the coordinate of maximum velocity depends on the fullness of the boundary part of the velocity profile and the co-current parameter m. For $w_0 = 0$ and $n = 1/7$, $\xi_m = 0.127$. This result corresponds to well-known theoretical and experimental data for submerged wall jets [8]. Inserting (1.4) into (1.3), we can also find the maximum velocity $w_m$ with allowance for wall friction.

We can use Eq. (1.3) to describe the profile of peripheral velocity in the jet. Thus, in the absence of rotation in the companion flow ($v_0 = 0$), the profile of peripheral velocity

$$v = v_{m0}\xi^n (b/\delta)^n (1 - \xi^{1,5})^2. \tag{1.5}$$

Here, v and $v_{m0}$ are the peripheral velocity at the point in question and the maximum value of peripheral velocity in the absence of momentum loss on the wall. In writing (1.5), we assumed that the thicknesses of the boundary layer $\delta$ and the jet b coincide for the circumferential and longitudinal directions.

We use (1.3) and (1.5) to find the distribution of the angle of twist of the flow, which is needed to analyze heat and mass transfer and friction:

$$\operatorname{tg}\varphi = \frac{v}{w} = \frac{v_{m0}}{w_{m0}}(1 - \xi^{1,5})^2 \Big/ \left[\left(1 - \frac{w_0}{w_{m0}}\right)(1 - \xi^{1,5})^2 + w_0/w_{m0}\right]. \tag{1.6}$$

The angle of twist of the flow on the wall ($\xi \to 0$)

$$\operatorname{tg}\varphi_w = v_{m0}/w_{m0}. \tag{1.7}$$

The distribution of the maximum value of the longitudinal $w_{m0}$ and peripheral $v_{m0}$ components of velocity along the surface in the flow can be found from the laws of conservation of linear and angular momenta. For an isothermal flow, these laws are written as

$$\int_R^{R\pm b} 2\pi w^2 r dr = \int_R^{R\pm s} 2\pi w_s^2 r dr + \int_{R\pm s}^{R\pm b} 2\pi w_0^2 r dr; \tag{1.8}$$

$$\int_R^{R\pm b} 2\pi v w r^2 dr = \int_R^{R\pm s} 2\pi v_s w_s r^2 dr. \tag{1.9}$$

Here and below, the top sign corresponds to flow about the cylinder, while the bottom sign corresponds to flow in the channel.

After jet profiles of the type (1.2) are inserted into Eqs. (1.8) and (1.9), the latter are easily integrated and yield theoretical formulas for the longitudinal component of velocity

$$\frac{w_{m0}}{w_s} = \frac{1}{m}\left\{1 - \frac{0.45 \pm 0.129b/R}{0.316 \pm 0.067b/R} + \sqrt{\left(\frac{0.45 \pm 0.129b/R}{0.316 \pm 0.067b/R}\right)^2 + \frac{s/b\,(m^2-1)\,(1 \pm s/2R)}{(0.316 \pm 0.067b/R)}}\right\} \tag{1.10}$$

and the angle of twist on the wall

$$\operatorname{tg}\varphi_w = \operatorname{tg}\varphi_s \left(\frac{w_s}{w_{m0}}\right)^2 \frac{s}{b}\left(1 \pm \frac{s}{R} + \frac{1}{3}\frac{s^2}{R^2}\right) \Big/ \Big[\Big(0.316 \pm \pm 0.133\frac{b}{R} + 0.0222b^2/R^2\Big) + (w_0/w_{m0})\,(0.134 \pm 0.126b/R + 0.0333b^2/R^2)\Big]. \tag{1.11}$$

The unknown quantity in (1.10) and (1.11) is the change in the width of the jet b over its length. This quantity is found below.

2. Laws of the Expansion of Twisted Wall Jets. According to [8], the equation which describes expansion of the jet has the form

$$db/dt = u', \tag{2.1}$$

where u' is the fluctuation velocity in the radial direction. For a flow in a centrifugal force field [5, 9]

$$u' = u_0' f. \tag{2.2}$$

Here, $u_0'$ is the fluctuation velocity in the radial direction in the absence of the effect of centrifugal forces. The value of $u_0'$ for a three-dimensional flow is determined by the shift in total velocity and with the assumption of similarity of the profiles of longitudinal and peripheral velocity

$$u_0' = \frac{l_0 |w|}{b} = c_0 \sqrt{(w_m - w_0)^2 + v_m^2} = c_0 |w_m - w_0| \sqrt{1 + \frac{\operatorname{tg}^2\varphi_s}{\left(1 - \frac{1}{m}\right)^2}} \tag{2.3}$$

($l_0 = c_0 b$ is the mixing length for the jet without twisting).

In Eq. (2.2), the function f considers the effect of centrifugal forces on the fluctuations of radial velocity. According to [9]

$$f = 1/\sqrt{1 + (y/l_0)^2 \mathrm{Ri}} \quad (\partial\Gamma/\partial r > 0); \tag{2.4}$$

$$f = \sqrt{1 - (y/l_0)^2 \mathrm{Ri}} \quad (\partial\Gamma/\partial r < 0). \tag{2.5}$$

The Richardson number, in (2.4), (2.5) characterizing the effect of centrifugal forces, has the form [5, 9]

$$\mathrm{Ri} = \left(\frac{2\Gamma}{r^3}\frac{\partial\Gamma}{\partial r} + \frac{1}{\rho}\frac{\partial\rho}{\partial r}\frac{\Gamma^2}{r^3}\right) \Big/ \left[\left(\frac{\partial w}{\partial r}\right)^2 + \left(\frac{1}{r}\frac{\partial\Gamma}{\partial r}\right)^2\right]. \tag{2.6}$$

($\Gamma = vr$ is the velocity circulation). For an isothermal wall jet, Eq. (2.6) becomes

$$\mathrm{Ri} = \pm 2\sin^2\varphi \frac{b}{R \pm b\xi}\frac{\omega}{\partial\omega/\partial\xi}, \quad \omega = w/w_m = v/v_m. \tag{2.7}$$

The experimental data [1] in Fig. 2 shows the ratio of the dimensionless fluctuation velocity for twisted and untwisted jets in the section $x/s \approx 20$, where the width of the jets is the same. Fluctuation velocity was normalized with regard to the modulus of the total velocity vector for the twisted jet in accordance with (2.3). For the untwisted jet, fluctuation velocity was normalized with regard to the excess longitudinal velocity $\Delta w_0 = w_m - w_0$.

The line shows the results of this calculation with (2.4), using Ri in the form (2.7). It can be seen that the theory correctly reflects the experimental data, which is evidence of the validity of the assumptions made as the basis of the transport model. Here, the centrifugal forces result in significant suppression of velocity fluctuations in the radial direction.

To integrate Eq. (2.1), it is necessary to obtain the effective value of Ri, which is independent of the transverse coordinate. The integral analog of Ri (2.7) will be

$$\langle \mathrm{Ri} \rangle = \pm A \sin^2 \varphi (b/R), \tag{2.8}$$

where A, as shown by the analysis, is a quantity which is weakly dependent on b/R and which we will assume to be constant. In the general case, this constant may be different for the external and internal flows.

Assuming that the angle of twist does not change along the jet and is equal to the angle of twist of the flow in a slit – which is sufficiently close to the experimental results in [1] – we obtain the law of jet expansion in the channel

$$\frac{b}{s} = \left\{ \left[ \frac{3A_1 \sin^2 \varphi_s J}{2R} + \left(1 + A_1 \sin^2 \varphi_s \frac{b_0}{R}\right)^{3/2} \right]^{2/3} - 1 \right\} \frac{R}{A_1 s \sin^2 \varphi_s}; \tag{2.9}$$

while the law for external flow of the jet about the cylinder

$$\frac{b}{s} = \left\{ \left[ \frac{A_2 \sin^2 \varphi_s J}{2R} + \left(1 + A_2 \sin^2 \varphi_s \frac{b_0}{R}\right)^{1/2} \right]^2 - 1 \right\} \frac{R}{A_2 s \sin^2 \varphi_s}. \tag{2.10}$$

In Eqs. (2.9) and (2.10)

$$J = 2c_0 s \sqrt{1 + \frac{\mathrm{tg}^2 \varphi_s}{(1 - 1/m)^2}} \int_0^{\bar{x}} \frac{|w_m - w_0|}{w_m + w_0} d\bar{x}, \quad \bar{x} = \frac{x}{s}. \tag{2.11}$$

As a first approximation, the value of $w_m$ can be calculated from the formula

$$(w_m - w_0)/(w_s - w_0) = c_1 (x/s)^{-0.5} \ (c_1 = 3.8), \tag{2.12}$$

which at $w_0 = 0$ becomes the well-known relation for submerged jets [10]. The applicability of (2.12) for twisted jets can be explained by the fact that, as shown by the experiments in [2, 11], twisting of the jet has little effect on maximum velocity. In sum, by inserting (2.12) into (2.11) and integrating the latter, we obtain

$$J = 2c_0 c_1 s \sqrt{1 + \frac{\mathrm{tg}^2 \varphi_s}{(1 - 1/m)^2}} |m - 1| \left( \sqrt{\bar{x}} - \frac{c_1 (m-1)}{2} \ln \frac{2\sqrt{\bar{x}} + (m-1) c_1}{c_1 (m+1)} - \frac{c_1 m}{m+1} \right). \tag{2.13}$$

Equations (2.9) and (2.10), together with (2.13), make it possible to calculate the jet expansion law and, after substitution into (1.10), (1.11), allow us to find the change in maximum velocity and angle of twist along the jet. Meanwhile, heat and mass transfer and friction can be determined from the solution of the corresponding integral relations of momentum or energy [12, 13]. It should be noted that for an untwisted jet ($\varphi_s = 0$), Eqs. (2.9), (2.10), and (2.13) change into the relation for a plane jet [8]

$$b/s = 2c_0 x/s + b_0/s \ (b_0 = s). \tag{2.14}$$

3. Discussion of Calculated Results. Comparison with Experimental Data. Calculations were performed within a broad range of $\varphi_s$ and m for the development of twisted jets in a channel and external flow about a cylinder. For comparison with these calculated results, we performed other calculations for two-dimensional untwisted wall jets using similar parameters for the companion flow. The turbulence constant $c_0$ was taken to be the same in each case and was equal to the value in the plane mixing layer ($c_0 = 0.11$ [8]). The parameter A in (2.10) and (2.11), characterizing the effect of centrifugal forces on turbulent transport processes, was given a value of 16. This resulted in fairly good agreement with the experimental data.

Figure 3a and b show the effect of the co-current parameter m on the law governing the change in maximum velocity and the character of expansion of walls jets, respectively, for a fixed distance from the edge of the slit x/s = 50. The solid lines show results calculated for the flow of twisted jets, while the dashed lines show results for untwisted jets. Curves

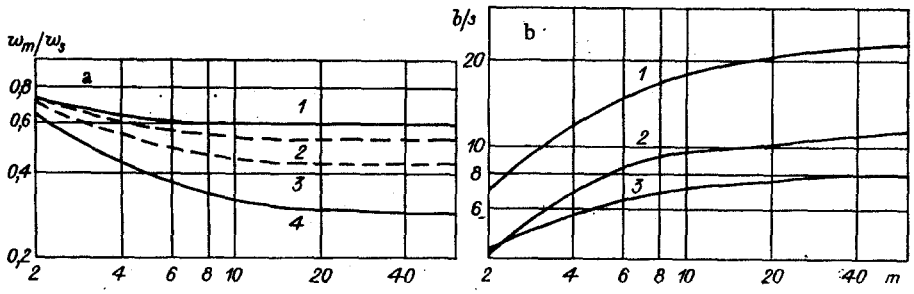


Fig. 3

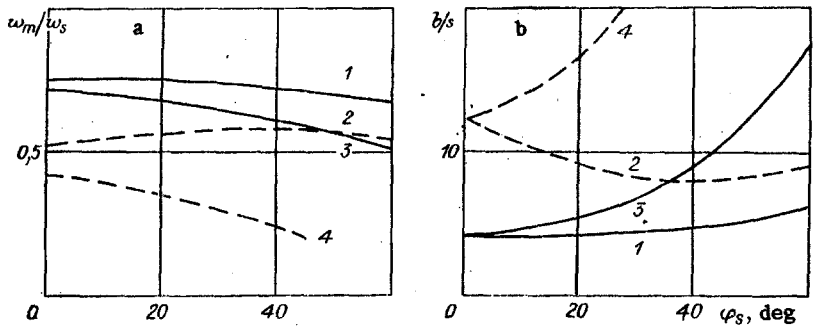


Fig. 4

1 and 2 correspond to flow in the channel, and curves 3 and 4 correspond to flow about the cylinder. The twisted jets were calculated for $\varphi_s = 30°$ . The co-current parameter typically has less effect on maximum velocity in the channel flow than in the flow about the cylinder. The data for the twisted and untwisted jets in the channel is similar. Here, in contrast to the external flow, the value of $w_m/w_s$ is higher for the twisted jet than the untwisted jet in the channel.

The co-current parameter also has a strong effect on width (Fig. 3b). Meanwhile, the width of the jet increases with an increase in the injection parameter. Curve 1 corresponds to twisted external flow ($\varphi_s = 30°$), 2 corresponds to untwisted external and internal flow, and 3 corresponds to twisted internal (channel) flow ($\varphi_s = 30°$). Twisting in the case of flow about the cylinder results in substantial expansion of the jet, while the internal jet becomes narrower if twisted at $m > 2.2$. This result is related to the effect of centrifugal forces on velocity pulsations in the radial direction.

Figure 4 shows the effect of $\varphi_s$ on the parameters of the wall jets. The calculations were performed for submerged jets ($m \to \infty$, dashed lines) and in the presence of a strong co-current flow ($m = 2$, solid lines). All of the data pertains to the section $x/s = 50$; 1 and 2 correspond to flow in the channel with $m = 2$ and $\infty$; 3 and 4 correspond to flow about the cylinder with the same co-current parameters.

It can be seen from Fig. 4a that the maximum velocity is less dependent on $\varphi_s$ for flow in the channel than for the flow about the cylinder. This is related to the fact that, for the channel flow, centrifugal forces and the increase in velocity resulting from twisting have opposite effects in regard to the expansion of the jet. In the flow about the cylinder, both of these effects lead to expansion of the jet (Fig. 4b).

In the above calculations analyzing the effect of twisting on the development of wall jets, we used velocity profile (1.3). This relation was checked in a comparison with experimental data on velocity profiles in untwisted and twisted wall jets. The test data on the profiles in a two-dimensional wall jet ($m = 9.17$), taken from [14], is shown in Fig. 5a: 1) $x/s = 9.6$; 2) 29; 3) 73; 4) 250; the distance from the wall is referred to the coordinate of half the maximum velocity, and the lines show results calculated from Eqs. (1.3), (1.10), and (2.13). It can be seen that the calculated results describe the experimental data well. A comparison with the test data in [15] on jet width and the change in maximum velocity also showed that this method for the most part accurately reflects the experimental findings within a broad range of m.

Figure 5b compares profiles of longitudinal velocity for a twisted jet [1] with calculated profiles in different sections of the channel, $\varphi_s = 52°$, 1) $x/s = 12.4$; 2) 20.5; 3)

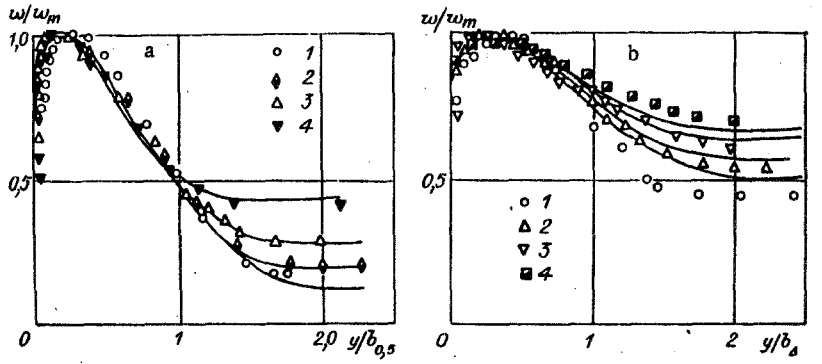


Fig. 5

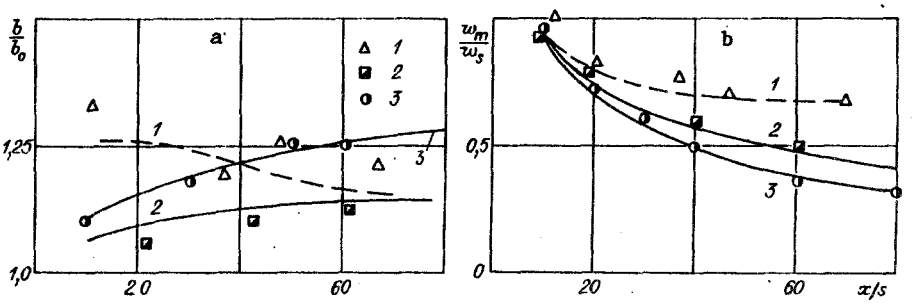


Fig. 6

36.8; 4) 47.3. The calculations were performed for a constant co-current parameter $m = w_m/w_0 = 2.2$. The agreement between theory and experiment can be considered satisfactory if we take into account that the co-current flow in the tests underwent a change in longitudinal velocity of about 20%.

Figure 6a and b shows data on the width of twisted jets and the change in maximum velocity. The experimental points and the corresponding theoretical curves were obtained under the following conditions: 1) $\varphi_s = 52°$, $m = 2.2$ (flow in channel [1]); 2) $\varphi_s = 13.7°$, $m = 6$; 3) $\varphi_s = 16.5$, $m \to \infty$ (flow about cylinder [11]).

The experimental results on the width of twisted jets in Fig. 6a are referred to the corresponding values for untwisted wall jets and the same co-current parameter. Such a treatment reveals the effect of twisting alone on the character of jet expansion. The line coinciding with the x-axis $b/b_0 = 1$ corresponds to flow of the untwisted jet. It is evident that twisting leads to more intensive expansion of the jet both inside the channel (points 1) and about the cylinder (points 2 and 3). However, in the external flow, the increase in $b/b_0$ along the flow is monotonic. In the case of the channel flow, there is a reduction in the relative width of the jet. This difference can be explained by the suppression of turbulent pulsations as a result of body forces in the external part of the jet.

As for untwisted jets, the maximum velocity is more conservative in regard to a change in the co-current parameter and twisting than is the width of the mixing layer. This is confirmed by the data in Fig. 6b for the injection parameter and angle of twist, which were varied within broad ranges. The theoretical curves in Fig. 6 were obtained from the formulas (1.3), (1.5), (1.6), (1.10), (1.11), (2.10), (2.11), (2.14). Meanwhile, the best agreement with the experiment is given by the value of the constant $c_0 = 0.14$ for channel flow and $c_0 = 0.09$ for flow about the cylinder. This fact probably reflects the effect of the propagation of annular axisymmetric jets. The same values of the constant were used in the calculations for twisted jets.

Thus, the method of calculation developed here makes it possible to determine the main characteristics of semi-infinite co-current twisted jets in channels and in flow about a cylinder. We established and analyzed the reasons for the effect of the companion flow, twisting, and centrifugal forces on turbulence parameters and the width of the mixing layer.

## LITERATURE CITED

1. É. P. Volchkov, S. Yu. Spotar', and V. I. Terekhov, Twisted Wall Jet in a Cylindrical Channel, Preprint ITF SO AN SSSR, Novosibirsk, No. 84-82 (1982).

2. É. P. Volchkov, S. Yu. Spotar', and V. I. Terekhov, "Turbulence characteristics of a bounded twisted jet," in: Wall Jets [in Russian], Novosibirsk (1984).
3. É. P. Volchkov, Wall Gas Screens [in Russian], Novosibirsk, Nauka (1983).
4. Z. B. Sakipov, Theory and Methods of Calculation of Semi-Infinite Jets and Condensed Jets [in Russian], Nauka, Alma-Ata (1978).
5. É. P. Volchkov, N. A. Dvornikov, and V. I. Terekhov, Heat and Mass Transfer and Friction in the Turbulent Boundary Layer of a Twisted Flow, Preprint ITF SO AN SSSR, Novosibirsk (1983), No. 107-83.
6. T. Karman, "Über laminare und turbulente Reilung," Zh. Angew. Math. Mech., 1, 233 (1921).
7. D. Wormley, "Analytical model of incompressible flow in short swirl chambers," Teor. Osn. Inzh. Raschetov, No. 2 (1969).
8. G. N. Abramovich, T. A. Girshovich, S. Yu. Krasheninnikov, et al. (eds.), Theory of Turbulent Jets [in Russian], Nauka, Moscow (1984).
9. N. A. Dvornikov and V. I. Terekhov, "Transfer of momentum and heat in a turbulent boundary layer on a curved surface," Zh. Prikl. Mekh. Tekh. Fiz., No. 3 (1984).
10. E. P. Volchkov, S. S. Kutateladze, and A. I. Leont'ev, "Interaction of a turbulent jet with a hard wall," Zh. Prikl. Mekh. Tekh. Fiz., No. 2 (1965).
11. I. I. Ibragimov and B. P. Ustimenko, "Study of the aerodynamics of a twisted jet developing along a cylindrical wall in a co-current flow," Probl. Teploenerg. Prikl. Teplofiz., No. 2 (1965).
12. N. A. Dvornikov and S. Yu. Spotar', "Heat and mass transfer in a twisted wall jet," in: Hydrogasdynamics and Heat Transfer in Condensed Media [in Russian], ITF SO AN SSSR, Novosibirsk (1981).
13. N. A. Dvornikov, "Turbulent heat transfer in a twisted wall jet," in: Current Problems of Thermophysics [in Russian], ITF SO AN SSSR, Novosibirsk (1984).
14. R. A. Seban and L. M. Back, "Velocity and temperature profiles in a wall jet," Int. J. Heat Mass Transfer, 3, No. 4 (1961).
15. V. Kruka and S. Eskinazi, "The wall jet in a moving stream," J. Fluid Mech., 20, Pt. 4 (1964).

# RADIAL OSCILLATIONS OF VAPOR–GAS BUBBLES

N. S. Khabeev

UDC 532.529

We are concerned with vapor–gas bubbles executing small radial oscillations in a liquid. The dynamics of vapor–gas bubbles has important bearing, in particular, on sound propagation in the top layer of the ocean. The description of the process in this situation is far more complicated than in the case of a gas bubble or a vapor bubble. The attenuation of sound in a liquid containing vapor–gas bubbles is clearly related to the decay rate of the radial pulsations of the bubbles.

Here we investigate the influence of interdiffusion of the components of a vapor–gas mixture on the decay rate of small oscillations of vapor–gas bubbles. We show that the addition of a minute quantity of an inert gas to a vapor bubble lowers the damping of the bubble oscillations significantly. We confirm the fact that the derived analytical relations are in good agreement with the experimental data on the damping of radial oscillations of gas and steam bubbles in water. We also discuss the linear radial pulsations of vapor–gas bubbles in a sound field. We derive asymptotic expressions for the bubble response function, which are valid for different frequency ranges. We compare these relations with the experimental data for steam–air bubbles in subcooled water and establish good agreement between them.

## 1. Fundamental Equations

The problem of spherically symmetric process around vapor–gas bubbles has been formulated previously [1, 2], and their small oscillations have been investigated in detail [3-5]. The system of equations describing linear radially symmetric oscillations of a bubble filled

Moscow. Translated from Zhurnal Prikladnoi Mekhaniki i Tekhnicheskoi Fiziki, No. 6, pp. 74-82, November-December, 1987. Original article submitted September 2, 1986.



0021-8944/87/2806-0870$12.50 